

Article

Characterization for Disposal of the Residues Produced by Materials Used as Solid Oxygen Carriers in an Advanced Chemical Looping Combustion Process

Adriana L. Carrillo ¹ and Carmen R. Forero ^{2,*} 

¹ School of Chemical Engineering, Universidad del Valle, Calle 13 No. 100-00, 760032057 Cali, Colombia; adriana.carrillo@correounivalle.edu.co

² Engineering School of Natural and Environmental Resources (EIDENAR), Universidad del Valle, Calle 13 No. 100-00, 760032057 Cali, Colombia

* Correspondence: carmen.forero@correounivalle.edu.co; Tel.: +57-2-3212100 (ext. 7018)

Received: 19 June 2018; Accepted: 13 July 2018; Published: 20 July 2018



Featured Application: (1) The residues of six low-cost materials found in Colombia were characterized with CH₄ and H₂ used as fuels in a chemical looping combustion (CLC) system. (2) The residues of the low-cost materials evaluated would not have a negative impact on the environment when disposed of in a landfill. (3) The residues are not considered toxic waste or dangerous according to current Colombian legislation or European regulations, respectively.

Abstract: Chemical looping combustion (CLC) is a technology that is part of the capture and storage of CO₂ through the combustion with solid oxygen carriers (OCs). It is considered an energy-efficient alternative to other methods, since it is a technology that inherently separates CO₂ and has the advantage of not requiring additional energy for this separation. The key to the performance of CLC systems is the OC material. Low-cost materials, i.e., natural minerals rich in metal oxides (chromite, ilmenite, iron, and manganese oxides) were used in this investigation. These may contain traces of toxic elements, making the carrier residues hazardous. Therefore, the oxidized and reduced-phase residues of six OCs, evaluated in a discontinuous batch fluidized bed reactor (bFB) using methane and hydrogen as the reducing gas, were characterized by several techniques (crushing strength, SEM, XRD, and XRF). The researchers found that, in general terms, the residues present a composition very similar to that reported in the fresh samples, and although they contain traces of Ba, Cu, Cr, Ni or Zn, these compounds do not migrate to the leachate. It was mainly found that, according to the current regulations, none of the residues are classified as toxic, as they do not exceed the permissible limits of metals (100 and 5 mg/L for Ba and Cr, respectively), with 3.5 mg/L the highest value found for Ba. Thus, they would not have a negative impact on the environment when disposed of in a landfill.

Keywords: low-cost oxygen carriers; carrier residues; environmental impact; leaching test

1. Introduction

The main contributors to global warming are power plants through the emission of greenhouse gases, especially CO₂, from the combustion of fossil fuels [1]. Recently, in the 21st United Nations conference on climate change (COP21), 195 countries attended with the aim of curbing CO₂ emissions in the atmosphere [2]. Several options are needed in order to minimize these medium-term emissions, including CO₂ capture and storage [3–5]. In this context, chemical looping combustion (CLC) is a promising technology to capture CO₂ at low economic and energy cost [6].

CLC is an advanced combustion technology which inherently separates CO₂. It includes the use of a metal oxide as an oxygen carrier (OC), which transfers oxygen to the fuel during combustion; therefore, direct contact between the fuel and the air is avoided. The most commonly proposed configuration is two interconnected fluidized bed reactors. The reduction reactor, in which the metal oxide is reduced upon reaction with the fuel and the oxidation reactor and where the reduced metal oxide is oxidized with air [7–9], has an outlet stream consisting of CO₂ and H₂O, while the output stream from the oxidation reactor contains N₂ and O₂ [10]. The net chemical reaction over the two reactors is the same as that in normal combustion with the same amount of heat released, but with an important difference: the carbon dioxide is inherently separated from the nitrogen, and no extra energy is required for this separation [6,10].

The review carried out by Adánez et al. [6] shows that studies carried out so far have synthesized more than 700 oxygen carriers, obtaining materials with promising characteristics in terms of reactivity and stability [11]. However, due to the high cost of synthetic materials, it would be less expensive to use minerals in their natural form or industrial waste. This would be very promising for use with solid and gaseous fuels [12–21]. In several areas of Colombia, metal oxides can be found in their natural form or as waste from industries and mining, which could be used in the implementation of CLC technology, or even in in situ gasification with CLC (iG-CLC) [22,23].

In the literature, chromite is the least studied material for use as an oxygen carrier. In Colombia, there are reports of chromite mineralization east of Medellín (deposits in Santa Elena); around Ituango, Yarumal, and Serranía de Baudó; and in the upper part of the Guapi river [24].

Ilmenite is an attractive low-cost material that could be used as an OC because it has a high CO conversion rate and a moderate CH₄ conversion rate [25]. Although the pre-oxidized and activated ilmenite initially presented low reactivity, after several redox cycles, it undergoes an activation process that increases its porosity and reactivity, notably when using H₂, CO, and CH₄ as fuels [6,26]. However, the segregation of Fe from TiO₂, causes the oxygen transport capacity to decrease after 100 redox cycles when solid fuel is used [27,28]. From the reduced ilmenite form (FeTiO₃) and the oxidized form (Fe₂TiO₅ + TiO₂), the reduction/oxidation of ilmenite is carried out. The probable intermediate phases of the reaction are Fe₂O₃, Fe₂O₃.TiO₂, though this does not totally exclude the presence of other intermediate stages [25].

Due to their low cost and environmental compatibility, iron-based carriers are considered an attractive option for applications with CLC technology [29], despite their weak redox characteristics, such as low methane conversion and low oxygen transport capacity [30]. In these carriers, different states of oxidation can be found when Fe₂O₃ is reduced to Fe₃O₄, FeO, or Fe. However, due to thermodynamic limitations, only the transformation of hematite (Fe₂O₃) to magnetite (Fe₃O₄) may be applicable in industrial CLC systems with an interconnected batch fluidized bed reactor configuration [30,31]. Promoting reductions to wüstite (FeO) or Fe would produce a considerable decrease in the purity of CO₂ obtained in the fuel reactor caused by the increase of the concentrations of CO and H₂ when methane is used [32]. In addition to the thermodynamic limitations mentioned, some authors have encountered problems of agglomeration in the bed, which is associated with the phase change from wüstite to magnetite during the oxidation stage in the air reactor [6,33–35]. Other chemical characteristics are advantageous when using these carriers, such as the low tendency to have carbon deposition and nonexistent risk of the formation of sulfide or sulfates due to the sulfur content in the combustible gas or the operating temperature [6,32,36].

As with iron-based carriers, special interest has been found in the literature in the study of manganese-based materials [15,18,23,37,38], bearing in mind that this metal oxide is considered an inexpensive and nontoxic material. In addition, the oxygen transport capacity is higher compared to iron-based compounds [6,15]. Several states of oxidation may be involved in the redox reactions of manganese. MnO₂ decomposes at a temperature of approximately 500 °C, while Mn₂O₃ is thermodynamically stable in the air at temperatures below 900 °C. However, at temperatures higher than 800 °C, only the Mn₃O₄ form is stable [39,40]. On the other hand, it has been found that manganese

ores show poor mechanical stability and poor fluidization properties, making them inadequate oxygen carriers [14]. It is also possible to find materials with combined oxides that can be used as OCs, such as manganese and silicon oxides. These are considered to be economical and of low impact to health and the environment [41,42]. In a kinetic study [22] comparing the activation energies and rate index (an important parameter that allows comparison of the reactivity of the OCs), manganese waste was the most reactive of the materials studied, followed by iron ore. Furthermore, the rate index found for the Mn waste was higher than that reported for similar materials in other studies [15,37,38]. The higher reactivity of Mn waste may be due to the formation of mixed Mn and Si oxides, such as braunite ($\text{Mn}_7\text{SiO}_{12}$) and rhodonite (MnSiO_3)—phases which are very important for the release of oxygen [43].

Among other important aspects considered when choosing the carrier is its environmental impact [6]. The Carboquímica Institute (Zaragoza, Spain) has worked on OC solid waste management, characterization, and layout. These studies analyzed the presence of hazardous metals in copper-based and iron-based OC residues previously used in a CLC system with methane and carbon, respectively. Researchers found that most of the residues were stable and non-reactive with low environmental impact, and they could therefore be disposed of in a landfill for nonhazardous waste [44,45]. In the two studies mentioned, a leaching test was performed according to the Spanish norm, UNE-EN-12457-3 [46], and the maximum limits allowed according to the standard established by the Council of the European Union, decision 2003/33/EC [47].

In this work, residues were obtained in a 500 Wth CLC plant operated with different low-cost OCs found in Colombia. The residues were characterized, and the environmental feasibility of the use of these materials was preliminarily determined based on whether the concentration of metals present in their leachates were in accordance with current regulations, both nationally and in Europe.

2. Materials and Methods

2.1. Materials

The OCs used in this study were low-cost materials that showed good performance in terms of oxygen transport capacity, kinetics, and reactivity, which were calculated by thermogravimetric analysis (TGA) in previous studies carried out at Universidad del Valle [48–50]. Table 1 shows the six materials selected for the present study and their characterization, which was performed by X-ray fluorescence (XRF), X-ray diffraction (XRD), and crushing strength analysis. The crushing strength of materials was measured with a Shimpo FGN-5X apparatus; the average value of 20 measurements was taken as the crushing strength.

2.2. Experimental Procedure

The six materials selected as OCs were evaluated in a discontinuous batch fluidized bed (bFB) prototype (Figure 1). The heart of the system is a discontinuous batch fluidized bed reactor (2) in which each of the oxygen carriers are charged and undergo purge-reduction-purge-oxidation cycles. The furnace (1) provides the heat necessary to reach the operating temperature and the heating is performed through electric resistors. The gas supply system (3) regulates nitrogen, air, fuel gas, and/or the mixtures required according to the needs of the process. At the outlet line of the reactor gases, there are two filters (4) for retaining the particulate matter (fines) entrained by the gases. The collection of the fines in these filters permits the calculation of the attrition rate, A (%/h), according to Equation (1), where p_f is the weight of elutriated particles $<40 \mu\text{m}$ during Δt , p_t is the total weight of the solids inventory, and Δt is the period of time during which the particles are collected [51].

$$A = \frac{p_f}{p_t \Delta t} * 100 \quad (1)$$

The gas conditioner (5) enables the particulate matter and moisture to be removed from the gases from the reactor prior to entering the gas analysis system (6), which enables the composition of the reactor outlet stream to be quantified.

Table 1. Characterization of low-cost oxygen carriers (OCs).

OC	CRSI003	FEMA004	FEMA011	ILME007	OXMN009	OXMN010A
Origin	Chromite Ore, Antioquia	Iron Ore, Antioquia	Iron Ore, Cauca	Ilmenite Ore, Antioquia	Manganese Ore, Valle	Manganese Waste, Nariño
Element	Composition (%) ^a					
Si	0.8	0.0	1.6	2.4	1.8	13.0
Al	3.5	0.9	0.4	0.5	0.2	2.5
Fe	27.2	41.5	65.9	30.7	1.0	3.5
Ca	0.2	0.3	0.8	0.9	0.5	1.9
Mg	2.8	1.3	0.1	0.3	0.1	0.8
Na	-	-	-	0.1	-	0.4
K	-	-	-	-	-	0.2
Cu	-	-	-	-	-	0.1
Zn	0.2	0.1	-	-	-	-
Ti	2.6	12.9	-	24.5	-	0.2
V	0.2	0.2	-	0.2	0.1	-
Cr	28.7	7.0	-	-	-	-
Ni	-	-	-	-	-	-
P	-	-	-	-	0.1	0.1
Mn	0.5	-	-	2.5	53.4	35.7
Ba	-	-	-	-	-	0.4
O	33.1	31.8	31.0	34.2	18.7	30.7
LOI ^b	0.0	0.6	0.0	3.5	23.1	10.3
Total	100.0	96.6	100.0	99.9	99.1	99.7
Crushing strength (N)	7.3	5.0	5.8	5.9	5.6	2.3
Crystalline phases	FeCr ₂ O ₄	Fe ₂ O ₃ , Fe ₃ O ₄ , FeTiO ₃ , FeCr ₂ O ₄	Fe ₃ O ₄ , Fe ₂ SiO ₄	Fe ₂ O ₃ , FeTiO ₃ , CaO	SiO ₂ , Mn ₃ O ₄	MnSiO ₃ , FeO
Density (kg/m ³)	4964	4943	3116	4639	3286	3009

^a Percentage in % w/w. Values less than 0.1 are negligible. ^b LOI: Loss on ignition.

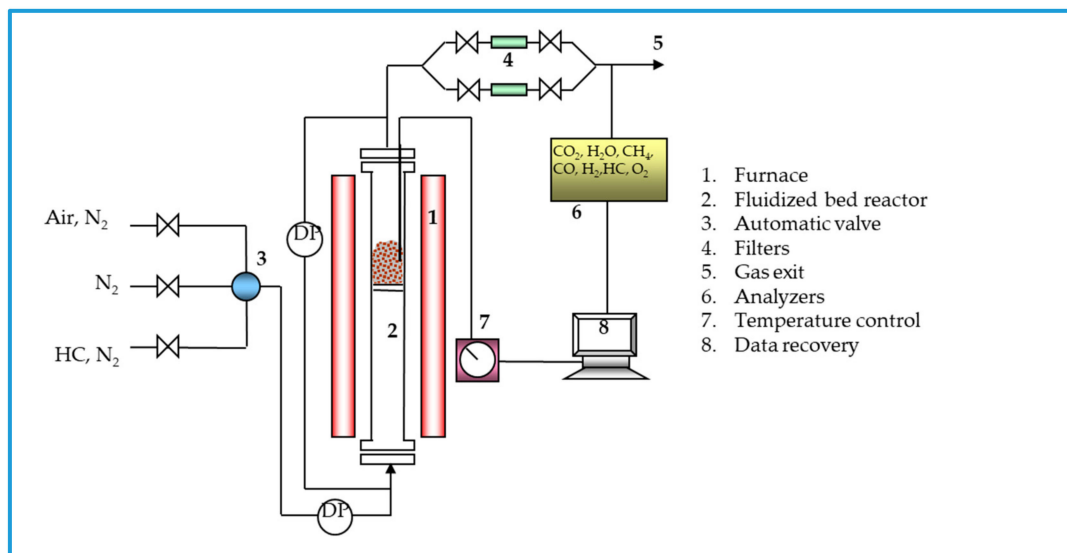


Figure 1. Diagram of the discontinuous chemical looping combustion (CLC) system.

The residues studied were collected from the reactor core in the last reduction and oxidation cycle. This operation was performed under the conditions summarized in Table 2.

Table 2. Operating conditions for obtaining residues.

Variable	Description
Temperature	950 °C
Number of cycles	30
Particle size	100–300 microns
Reducing gas	H ₂ (25%)–N ₂ (75%), CH ₄ (20%)–N ₂ (80%)
Oxidizing gas	100% air
Flow (l/h)	>2 × minimum fluidization velocity (>2 × U _{mf})
Weight OC (g)	300

All oxygen transporters were evaluated using hydrogen as the reducing gas in the proportions described in Table 2; in addition, the materials FEMA011 and OXMN010A were evaluated using methane. Thirty cycles were performed for each experiment. The material was heated in an air atmosphere until 950 °C; between reduction and oxidation periods, a purge was carried out with N₂ for 2 min to prevent contact between the fuel and the air.

2.2.1. Characterization of OC Residues

In total, 16 residues were characterized using different techniques: crushing strength analysis, morphological characterization using a scanning electron microscope (SEM), identification of crystalline phases by X-ray diffraction (XRD), and elemental analysis by X-ray fluorescence (XRF).

In the crushing strength analysis, 20 measurements per sample were taken using the Shimpo FGN-5X dynamometer. The identification of crystalline phases by XRD was performed to compare the phases present in the oxidized and reduced states of each sample in order to predict the reactions that were carried out in the reactor. Using the scanning electron microscope (SEM) Jeol JSM6490LV, the particle morphology of the OC residues was observed and compared with the original material. XRF analysis was performed in order to quantify the elemental composition of the residues.

2.2.2. Leaching Behavior Tests

Finally, the leaching test—toxicity characteristic leaching procedure (TCLP)—was performed according to the standards in resolution 0062-2007 of the IDEAM [52]. The leach test was carried out at room temperature by contacting 80 g of sample with an amount of extraction fluid equal to 20 times the weight of the dried residue for 18 ± 2 h at frequency of 30 ± 2 rpm. The extraction fluid was prepared by diluting 5.7 mL of concentrated glacial acetic acid (17.5 M) in 500 mL of reagent grade water, adding 64.3 mL of 1 M NaOH, and gauging it to a liter (pH 4.93 ± 0.05). After the extraction period, 0.8 µm glass fiber filter paper was used to separate the solid from the liquid extract (leachate). After the extraction procedure, the presence of the metals (Ba, Cu, Cr, Ni, Zn) in the leachate was analyzed using the atomic absorption technique. According to current regulations [53], there are more than 30 contaminants (organic and inorganic) whose presence in a residue can render it toxic and therefore dangerous. However, taking into account previous research in this area, as well as the characterization of materials used as oxygen carriers (Table 1), the study was restricted to the possible toxicity of some of the metals present in the residues.

The metals to be analyzed were defined taking into account those that (1) were included as contaminants in the decree that regulates the prevention and management of hazardous waste [53], and (2) will additionally be found in the elemental composition of the original materials (Table 1). According to these criteria, it was established that the metals to be studied would be Ba and Cr. Since previous investigations of this subject were carried out under European Union standards, those metals covered by decision 2003/33/CE were also considered [47]. Therefore, Cu, Zn, and Ni were also analyzed for residues whose elemental composition (Table 1) indicates the presence of these metals.

One of the aspects that must be taken into account when considering a scaling of this technology is the disposal of solid residues generated due to loss of the oxygen carrier (generation of fines) and

to the life cycle of the material. It is necessary to keep in mind that a decisive factor when assessing the feasibility of using a carrier in the CLC process is whether its residues show a high potential for polluting the environment or are dangerous to health. Before considering the disposal of OC residues directly in a landfill, it is necessary to ensure that it is not hazardous waste and, therefore, that it does not exhibit any of the following characteristics: corrosive, reactive, explosive, toxic, flammable, infectious, or radioactive. Hazardous waste requires special and differential management compared to nonhazardous waste, because of the risk they pose to health and the environment [54].

3. Results and Discussion

3.1. Attrition

The attrition—known as the process of fragmentation that produces elutriation of the system particles [6]—is reported in Table 3 with the performance times for each material.

The FEMA011 and OXMN010A materials evaluated with methane presented a higher attrition rate, which would represent on an industrial scale a greater consumption of the carrier and a greater generation of solid residues. However, the attrition rates of some of the low-cost materials studied are comparable to those obtained with synthetic materials in previous studies [6].

The operating times in all cases were short, therefore, it is recommended to evaluate this property for longer periods in order to determine the attrition over time.

Table 3. Discontinuous batch fluidized bed (bFB) operating times to obtain waste and attrition.

Waste from OC	Reducing Gas	Operation Time (h)	Attrition Rate (%/h)
CRSI003	H ₂	8.3	0.0027
FEMA004	H ₂	7.8	0.0074
FEMA011	H ₂	7.3	0.2007
FEMA011	CH ₄	3.7	0.4156
ILME007	H ₂	6.5	0.0008
OXMN009	H ₂	4.1	0.0653
OXMN010A	H ₂	9.1	0.0059
OXMN010A	CH ₄	4.5	0.1506

3.2. Crushing Strength

Figure 2 shows the average measurements taken for different samples of each carrier (fresh, reduced, oxidized). The materials OXMN009 and FEMA011 have a lower crushing strength, greater than 2N in all cases. This is the limit value, according to the literature [55], for use as an oxygen carrier in a CLC system without having to undergo a calcination process to improve its mechanical properties. Additionally, when comparing the crushing strength of the oxidized and reduced phases, no significant differences were observed for any of the residues.

An increase in the resistance of materials FEMA004, ILME007, and CRSI003, with respect to fresh material, was observed, which can be associated with the effect of the operating temperatures (950–1000 °C) in the batch fluidized bed reactor. This is close to the calcination temperature (1100 °C) proposed by the literature [55]. Although all materials were subjected to the same operating temperatures, the same behavior was not observed for all residues, since the crushing strength of the OXMN009 material remained more or less constant, while the FEMA011 material was the only one that showed a decrease of that property.

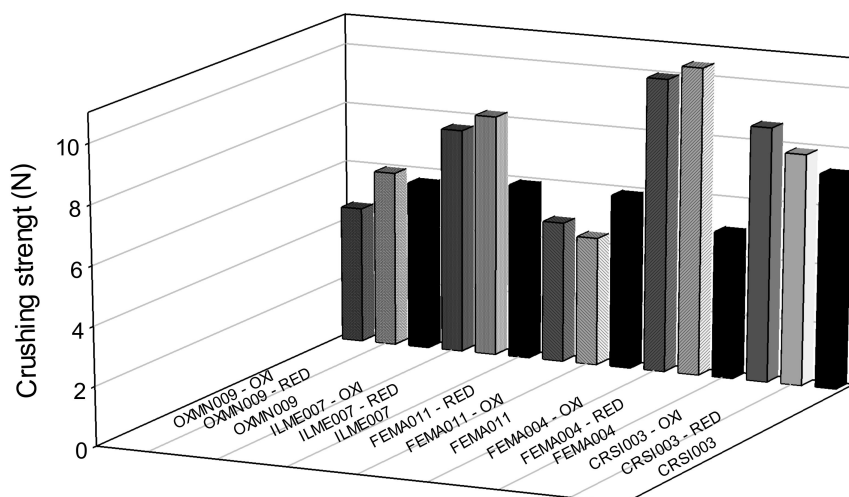


Figure 2. Crushing strength.

3.3. Crystalline Phases

In Table 4, the crystalline phases found in the reduced and oxidized residues of OCs and possible reactions are reported. The reported crystalline phases are not exclusive, so the existence of others not reported by the equipment is probable, since the software used did not identify some of the peaks of the diffractograms. In addition, when analyzing this type of sample, where different compounds exist, it is possible that the peaks overlap, thus preventing identification of any of them.

In the literature, there are no chromite reduction oxide reactions described. However, the crystalline phases identified in the oxidized residue of CRSI003 indicate that the active phase corresponds to iron oxide. On the other hand, no chromium oxides were present in the oxidized state, since Cr(III) is not oxidized to Cr(VI) at temperatures lower than 1200 °C. However, this reaction can be favored at temperatures between 600 and 900 °C due to the presence of alkalis (Na, K) and alkaline earth (Ca, Mg) metals [56].

In the oxidized residue of FEMA004, only Fe_2O_3 was identified, corresponding to the Oxidation Reaction 7. However, the oxidation of ilmenite (FeTiO_3) to pseudobrookite (Fe_2TiO_5) according to Reaction 5 was not identified. While analyzing the diffractogram of this pure compound (Fe_2TiO_5), it can be observed that it comes close to the unidentified peaks in the diffractogram of oxidized FEMA004 residues. For FEMA011 residues evaluated with H_2 gas and CH_4 , the oxidation reactions 6, 7, and 8 were theoretically expected and, according to XRD, the hematite and magnetite analyses were the only two crystalline phases identified in the residues evaluated with the two reducing gases.

The phases identified in the oxidized state of ILME007 indicate that reactions 4 and 5 occurred, however, no wüstite (FeO) or magnetite (Fe_3O_4) from the reduction of hematite (Fe_2O_3) was found as indicated by reactions 2 and 6. The diffractogram of the reduced sample could not be fully identified. Based on the chemical balance calculations provided by the HSC Chemistry software 6.1, it follows that the unidentified phases may be Fe_3O_4 , $\text{TiO}_2(\text{A})$, Fe_2TiO_5 , and/or FeO .

The material OXMN009 is constituted by more than 90% Mn_3O_4 , it is therefore expected that the crystalline phases would be present in reactions 9 and 10; nevertheless, Mn_3O_4 and Mn_2O_3 can be identified in the oxidized state residues. According to the literature, the latter compound is not stable at temperatures higher than 900 °C [39]. In spite of the above, according to the chemical balance calculations provided by HSC Chemistry software 6.1, it is possible to find Mn_2O_3 in the operating conditions used, while taking into account that Mn_3O_4 is an intermediate phase in the reduction/oxidation reactions between Mn_2O_3 and MnO . Consequentially, the presence of Mn_2O_3 suggests that reaction 10 was carried out until the formation of Mn_2O_3 .

Table 4. Crystalline phases in reduced and oxidized OC residues.

Residue/Gas	Oxidation State	Crystalline Phases	Possible Reactions		
CRSI003 H ₂	Reduced	-	$\text{Fe}_2\text{O}_3 + \text{H}_2 \rightarrow 2\text{FeO} + \text{H}_2\text{O}$	(2)	[16]
	Oxidized	$\text{Fe}_2\text{O}_3, \text{TiO}_2, \text{SiO}_2, \text{FeCr}_2\text{O}_4$	$4\text{FeO} + \text{O}_2 \rightarrow 2\text{Fe}_2\text{O}_3$	(3)	[16]
FEMA004 H ₂	Reduced	$\text{Fe}_2\text{O}_3, \text{Fe}_3\text{O}_4, \text{FeTiO}_3$	$\text{Fe}_2\text{TiO}_5 + \text{TiO}_2 \rightarrow \text{H}_2\text{FeTiO}_3 + \text{H}_2\text{O}$ $4\text{FeTiO}_3 + \text{O}_2 \rightarrow 2\text{Fe}_2\text{TiO}_5 + 2\text{TiO}_2$	(4) (5)	[16] [16]
	Oxidized	Fe_2O_3	$6\text{Fe}_2\text{O}_3 + 2\text{H}_2 \rightarrow 4\text{Fe}_3\text{O}_4 + 2\text{H}_2\text{O}$ $4\text{Fe}_3\text{O}_4 + \text{O}_2 \rightarrow 6\text{Fe}_2\text{O}_3$	(6) (7)	[14] [14]
FEMA011 CH ₄	Reduced	$\text{Fe}_2\text{O}_3, \text{Fe}_3\text{O}_4$	$6\text{Fe}_2\text{O}_3 + 1/2 \text{CH}_4 \rightarrow 4\text{Fe}_3\text{O}_4 + 1/2 \text{CO}_2 + \text{H}_2\text{O}$	(8)	[14]
	Oxidized	$\text{Fe}_2\text{O}_3, \text{Fe}_3\text{O}_4$	$4\text{Fe}_3\text{O}_4 + \text{O}_2 \rightarrow 6\text{Fe}_2\text{O}_3$	(7)	[14]
FEMA011 H ₂	Reduced	$\text{Fe}_2\text{O}_3, \text{Fe}_3\text{O}_4$	$6\text{Fe}_2\text{O}_3 + 2\text{H}_2 \rightarrow 4\text{Fe}_3\text{O}_4 + 2\text{H}_2\text{O}$	(6)	[14]
	Oxidized	$\text{Fe}_2\text{O}_3, \text{Fe}_3\text{O}_4$	$4\text{Fe}_3\text{O}_4 + \text{O}_2 \rightarrow 6\text{Fe}_2\text{O}_3$	(7)	[14]
ILME007 H ₂	Reduced	$\text{FeTiO}_3, \text{TiO}_2$	$\text{Fe}_2\text{TiO}_5 + \text{TiO}_2 + \text{H}_2 \rightarrow 2\text{FeTiO}_3 + \text{H}_2\text{O}$	(4)	[16]
	Oxidized	$\text{Fe}_2\text{O}_3, \text{TiO}_2, \text{SiO}_2, \text{Fe}_2\text{TiO}_5$	$4\text{FeTiO}_3 + \text{O}_2 \rightarrow 2\text{Fe}_2\text{TiO}_5 + 2\text{TiO}_2$	(5)	[16]
OXMN009 H ₂	Reduced	-	$\text{Mn}_3\text{O}_4 + \text{H}_2 \rightarrow 3\text{MnO} + \text{H}_2\text{O}$	(9)	[15]
	Oxidized	$\text{Mn}_3\text{O}_4, \text{Mn}_2\text{O}_3$	$12\text{MnO} + 2\text{O}_2 \rightarrow 4\text{Mn}_3\text{O}_4$	(10)	[15]
OXMN010 CH ₄	Reduced	$\text{SiO}_2, \text{MnSiO}_3, \text{SiO}_2, \text{FeO}, \text{Mn}_2\text{SiO}_4$	$2/3\text{Mn}_7\text{SiO}_{12} + 4\text{SiO}_2 \rightarrow 14/3\text{MnSiO}_3 + \text{O}_2$	(11)	[27]
	Oxidized	$\text{SiO}_2, \text{MnSiO}_3, \text{SiO}_2$	$10/3\text{MnSiO}_3 + 2/3\text{Mn}_7\text{SiO}_{12} \rightarrow 4\text{Mn}_2\text{SiO}_4 + \text{O}_2$	(12)	[27]
OXMN010 H ₂	Reduced	$\text{SiO}_2, \text{Mn}_2\text{SiO}_4, \text{Mn}_2\text{O}_3, \text{MnO}$	$\text{Mn}_3\text{O}_4 + \text{H}_2 \rightarrow 3\text{MnO} + \text{H}_2\text{O}$ $12\text{MnO} + 2\text{O}_2 \rightarrow 4\text{Mn}_3\text{O}_4$	(9) (10)	[15] [15]
	Oxidized	$\text{SiO}_2, \text{Mn}_3\text{O}_4, \text{Mn}_2\text{O}_3, \text{MnFe}_2\text{O}_4$	$2/3\text{Mn}_7\text{SiO}_{12} + 4\text{SiO}_2 \rightarrow 14/3\text{MnSiO}_3 + \text{O}_2$	(11)	[27]
			$10/3\text{MnSiO}_3 + 2/3\text{Mn}_7\text{SiO}_{12} \rightarrow 4\text{Mn}_2\text{SiO}_4 + \text{O}_2$	(12)	[27]

Finally, the fresh OXMN010A material is composed mainly of rhodonite (MnSiO_3) and a small percentage of wüstite (FeO). This silicon and manganese oxide (MnSiO_3) has been studied in CLC technology as an OC with oxygen decoupling (CLOU) [41,42], and reactions 11 and 12 are expected according to the literature. In the residues of the material OXMN010A evaluated with methane gas, no braunite was present ($\text{Mn}_7\text{SiO}_{12}$), but the oxidized crystalline phase of rhodonite and tephroite (Mn_2SiO_4) was detected. When analyzing the diffractograms of braunite and the tephroite, it was found that the main peaks of braunite are very close to the peaks present in tephroite, thus, an overlap of the peaks could be present, impeding the identification of $\text{Mn}_7\text{SiO}_{12}$. On the other hand, the presence of tephroite (Mn_2SiO_4) in the reduced state of the residues of OXMN010A evaluated with H_2 suggests that the oxygen decoupling reaction 12 was carried out and, as in the results obtained with methane, no braunite was identified ($\text{Mn}_7\text{SiO}_{12}$). On the other hand, the presence of MnO in the reduced state indicates that, in addition to reaction 12, reactions 9 and 10 were carried out between Mn_3O_4 and MnO .

In order to establish the reactions exactly, it is necessary to know the XRD results of the reduced samples of CRSI003 and OXMN009, but these could not be analyzed due to their mechanical characteristics, which prevented the sample from being pressed for reading.

3.4. Morphological Behaviour

Table 5 presents the scanning electron microscopy (SEM) results for both the fresh OCs and the residues obtained after testing in the bFB with H_2 or CH_4 .

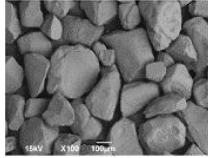
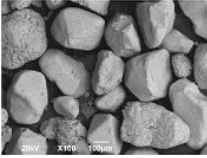
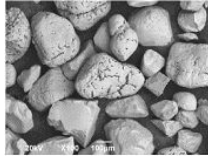
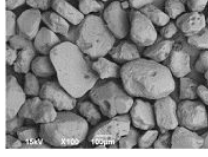
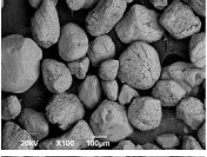
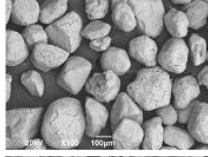
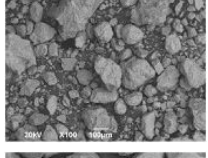
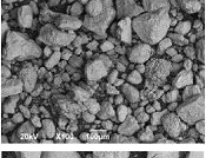
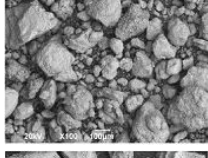
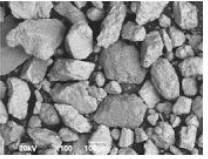
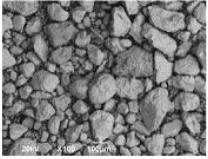
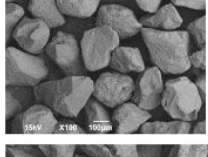
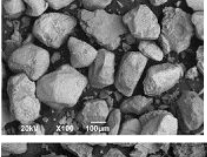
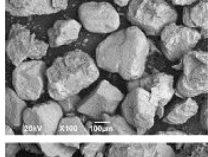
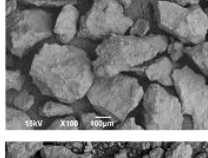
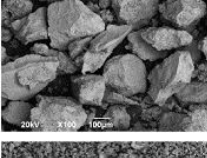
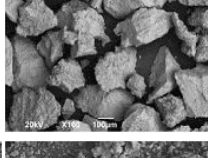
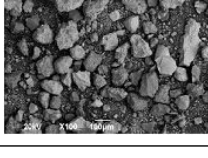
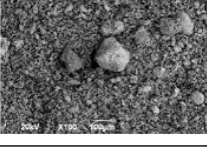
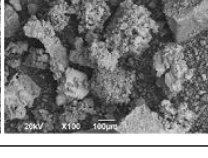
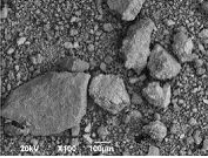
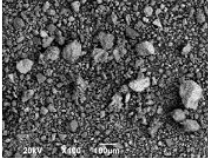
The main morphological changes observed in the oxidized and reduced states of the residues, with respect to the fresh material, are generally: a decrease of the particle size, generating a heterogeneous size; transformation of the smooth surface of the particles to a rough, porous surface with furrows. This is associated with the effect of friction and wear of the material when subjected to the CLC operation in the bFB.

A possible agglomeration was only observed in the particular case of OXMN010A with H_2 . However, the morphological changes of the particles were not of equal intensity for all the materials; greater changes in the morphology and integrity in the residues of OXMN010A were observed. Contrary to the above, the material OXMN009 maintained greater integrity of its particles after being subjected to the operation in the bFB. In an intermediate position, the residues of the materials FEMA004, CRSI003, and ILME007 were found, which presented some minor changes.

3.5. Elementary Composition Using XRF

According to the characterization by X-ray fluorescence (XRF) of the residues, it was found that the residues of the CRSI003 material are mainly composed of Fe and Cr at very similar percentages ($\approx 28\%$) with small amounts of Si, Al, Ca, Mg, Ti, and Mn. The main component in the residues of FEMA004 is Fe ($\approx 42\%$), followed by Ti ($\approx 14\%$) and Cr ($\approx 6\%$), as well as Mn, Si, Al, Ca, and Mg in small amounts. On the other hand, in the residues of the material FEMA011, the main element is Fe ($\approx 66\%$) and small quantities of Si, Al, Ca, and Mg can be found in its composition. The ILME007 residues are composed of Fe ($\approx 32\%$) and Ti ($\approx 25\%$) mainly, with small percentages of Si, Al, Ca, Mg, Na, and Mn. Mn ($\approx 53\%$) is the main element present in the residues of OXMN009, followed by percentages lower than 3% of Si and Fe, with very small amounts of Al, Ca, Mg, and P. Finally, in the residues of OXMN010A, Mn ($\approx 37\%$) is also present as the main component, but, unlike OXMN009, silicon is present in larger quantities—close to 20%—as well as small amounts of P, Al, Ca, Mg, Na, and K, along with Cu, Ti, and Zn. It was observed that, in general terms, the residues present a composition very similar to that reported in the fresh samples (Table 1), except for OXMN009 and OXMN010A, which present higher percentages. This can be explained by their high loss on ignition (LOI) content, which is burned in the first cycle.

Table 5. SEM results of oxygen carriers.

OC	Fresh	Reduced	Oxidized	Reduced	Oxidized
Gas		H ₂	H ₂	CH ₄	CH ₄
CRSI003					
FEMA004					
FEMA011					
ILME007					
OXMN009					
OXMN010A					

3.6. Hazardous Metal Leaching and Identification Test

Of the analyzed metals (Ba, Cu, Cr, Ni, and Zn), only the presence of Ba and Cr are considered toxic, under Colombian legislation for classifying a residue, if it exceeds the established maximum limit. In addition, according to the same legislation [53], wastes containing copper and zinc are considered to be hazardous waste, unless they do not show any of the following characteristics: corrosive, reactive, flammable, explosive, radioactive, infectious, toxic. Taking into account the origin of the materials and their characterization, it follows that the residues do not possess radioactive or infectious characteristics; additionally, according to the pH—between 6.6 and 11 in all cases—it is affirmed that they are not corrosive. Tests for reactivity, flammability, or explosivity are described in resolution 0062-2007 [52], which allow these characteristics to be determined for a material, and these tests are recommended for future studies.

Table 6 presents the concentration of metals that could be considered toxic that were in the leachate, as obtained through TCLP analysis on the residues, and the maximum limits allowed under Colombian legislation. The presence of Ba, Cu, Cr, Ni, or Zn in the leachates at the concentrations reported in Table 6 do not classify any of the residues evaluated as toxic, since they do not exceed the maximum values permitted (100 and 5 mg/L for Ba and Cr, respectively), with 3.5 mg/L the highest value found for Ba. However, based on the same regulations, it should be ruled out that the residues do not present any of the other hazardous characteristics mentioned above in order to ensure that they are nonhazardous waste and, therefore, that it is not necessary to resort to special treatment before their final disposal.

Table 6. Concentration of metals in the leachate of OC residues and maximum values allowed by Colombian regulations (Decree 4741. 1-27, 2005).

Max. Allowed	Ba	Cu	Cr	Ni	Zn
Decree 4741 (mg/L)	100	-	5	-	-
CRSI003 RED H ₂	0.421	-	<0.01	0.049	3.625
CRSI003 OXI H ₂	0.182	-	0.137	0.011	0.281
FEMA004 RED H ₂	-	0.139	<0.009	0.027	0.674
FEMA004 OXI H ₂	-	0.136	<0.007	0.006	0.426
FEMA011 RED H ₂	-	<0.004	<0.005	≈0	-
FEMA011 OXI H ₂	-	<0.007	<0.011	0.339	-
FEMA011 RED CH ₄	-	0.158	<0.009	0.098	-
FEMA011 OXI CH ₄	-	0.197	<0.009	0.040	-
ILME007 RED H ₂	-	-	<0.008	0.019	0.596
ILME007 OXI H ₂	-	-	<0.008	0.009	0.738
OXMN009 RED H ₂	3.447	0.010	0.086	0.026	0.127
OXMN009 OXI H ₂	2.107	<0.008	0.119	0.026	0.350
OXMN010A RED H ₂	0.816	0.054	<0.006	0.291	0.230
OXMN010A OXI H ₂	1.829	0.225	0.558	0.030	0.559
OXMN010A RED CH ₄	0.429	<0.006	0.351	≈0	<0.001
OXMN010A OXI CH ₄	1.591	<0.005	0.274	≈0	<0.001

On the other hand, with the intention of coming close to the European regulations for hazardous waste (Decision 2003/33/EC) [47], the results obtained were compared with the maximum allowances foreseen in said legislation for inert and nonhazardous waste. Without forgetting that the conditions of the leaching test are different in the two methods, i.e., resolution 0062-2007 [52] and UNE-EN-12457-3 [46]. According to the above, with respect to the European regulations, only an approximation of the characterization of the residues analyzed in this project is presented (Table 7). In addition to the time and the liquid to solid (L/S) ratio, one of the main differences between the two methods is the extraction fluid used, one being water in the European norm and the other being the fluid used in the Colombian norm, which is a mixture with a pH of approximately 4.9 (water + acetic acid + NaOH).

Regarding the effect of the pH of the extraction fluid, it is known that the solubility of inorganic compounds is strongly influenced by the pH and the redox potential, while that of organic compounds is dictated by polarity. According to the robustness analyses using the TCLP method, described in resolution 0062-2007, the acidity of the extraction fluid has a high impact on the extraction of metals, meaning that the lower the pH of the extraction fluid, the higher the extraction [52].

The maximum permissible values reported in Table 7 were extrapolated for an L/S = 20 ratio (ratio used in the leaching test performed in the present investigation), taking into account that the European standard prescribes values for L/S ratios of 2 and 10. According to the results presented in Table 7, none of the residues could be classified as inert waste; however, all would be classified as nonhazardous waste.

These results are very important, mainly for FEMA011 and OXMN010A, which have shown great potential for use in CLC and iG-CLC technologies [22,23].

Table 7. Concentration of metals in the leachate of OC residues and maximum values allowed by European regulations (Decision 2003/33/EC).

Max. Allowed (mg/kg Dry Matter)	Ba	Cu	Cr	Ni	Zn
Inert Waste	36.25	3.375	0.875	0.65	6.5
Non-Hazardous Waste	187.5	81.25	17.5	16.25	81.25
CRSI003 RED H ₂	8.421	-	<0.2	0.981	72.500
CRSI003 OXI H ₂	3.646	-	2.748	0.212	5.624
FEMA004 RED H ₂	-	2.790	<0.18	0.535	13.477
FEMA004 OXI H ₂	-	2.719	<0.14	0.115	8.517
FEMA011 RED H ₂	-	<0.08	<0.1	≈0	-
FEMA011 OXI H ₂	-	<0.14	<0.22	6.785	-
FEMA011 RED CH ₄	-	3.160	<0.18	1.965	-
FEMA011 OXI CH ₄	-	3.933	<0.18	0.807	-
ILME007 RED H ₂	-	-	<0.16	0.382	11.917
ILME007 OXI H ₂	-	-	<0.16	0.172	14.754
OXMN009 RED H ₂	68.947	0.197	1.727	0.525	2.536
OXMN009 OXI H ₂	42.135	<0.16	2.388	0.510	6.994
OXMN010A RED H ₂	16.319	1.075	<0.12	5.813	4.598
OXMN010A OXI H ₂	36.587	4.500	11.160	0.605	11.183
OXMN010A RED CH ₄	8.589	<0.12	7.029	≈0	<0.02
OXMN010A OXI CH ₄	31.820	<0.1	5.471	≈0	<0.02

4. Conclusions

Based on the results, the residues of the low-cost oxygen carriers evaluated in the present investigation would not have a negative impact on the environment when disposed of in a landfill, because they are not considered toxic waste according to the Colombian legislation currently in force, or dangerous according to European regulations. Therefore, it is preliminarily concluded that, in environmental terms, it is feasible to use low-cost materials, i.e., natural minerals rich in metal oxides (chromite, ilmenite, iron, and manganese oxides) as industrial-scale oxygen carriers.

For iron and manganese ores, these results, together with studies showing their high reactivity, ensure that CO₂ capture using these materials will not generate health or environmental problems.

Author Contributions: A.L.C. and C.R.F. conceived and designed the experiments; A.L.C. performed the experiments; A.L.C. and C.R.F. analyzed the data; C.R.F. contributed reagents/materials/analysis tools; A.L.C. and C.R.F. wrote the paper.

Acknowledgments: This research was conducted with financial support from the Unión Temporal Incombustión (Temporary Joint Working Group) and Colciencias through the Contract of Contingent Recovery RC 0852-2012. Adriana Carrillo thanks the Union Temporal Incombustión for the economic support with the studies in the Chemical Engineering Master's program. Thanks to Instituto de Carboquímica for the support provided, allowing

the investigation to use the Shimpo FGN-5X dynamometer to perform crushing resistance analysis and HSC Chemistry software 6.1 to evaluate the chemical equilibrium.

Conflicts of Interest: The authors declare no conflict of interest.

References

1. International Energy Agency (IEA). *International Energy Outlook 2016*; IEA: New York, NY, USA, 2016.
2. UNFCCC. *Conferencia de las Partes 21 Periodo de Sesiones Cop 21, París del 30 de Noviembre al 11 de Diciembre del 2015*; Convención Marco de las Naciones Unidas Sobre Cambio Climático: Paris, France, 2015.
3. IPCC. *Special Report on Carbon Dioxide Capture and Storage*; Prepared by Working Group III of the Intergovernmental Panel on Climate Change; Metz, B., Davidson, O., de Coninck, H.C., Loos, M., Meyer, L.A., Eds.; Cambridge University Press: Cambridge, UK; New York, NY, USA, 2005; p. 442.
4. Institute, G.C. *The Global Status of CCS: 2016 Summary Report*; Global Carbon Capture and Storage Institute Ltd: Melbourne, Australia, 2016.
5. International Energy Agency (IEA). *Energy Technology Perspectives 2016*; IEA: Paris, France, 2016.
6. Adanez, J.; Abad, A.; Garcia-Labiano, F.; Gayan, P.; de Diego, L.F. Progress in chemical-looping combustion and reforming technologies. *Prog. Energy Combust. Sci.* **2012**, *38*, 215–282. [[CrossRef](#)]
7. Ishida, M.; Jin, H. A new advanced power-generation system using chemical-looping combustion. *Energy* **1994**, *19*, 415–422. [[CrossRef](#)]
8. Lyngfelt, A.; Leckner, B.; Mattisson, T. A fluidized-bed combustion process with inherent CO₂ separation; application of chemical-looping combustion. *Chem. Eng. Sci.* **2001**, *56*, 3101–3113. [[CrossRef](#)]
9. Leion, H.; Mattisson, T.; Lyngfelt, A. The use of petroleum coke as fuel in chemical-looping combustion. *Fuel* **2007**, *86*, 1947–1958. [[CrossRef](#)]
10. Mattisson, T.; Lyngfelt, A. Applications of Chemical Looping Combustion with Capture of CO₂. In *Second Nordic Minisymposium on Carbon Dioxide Capture and Storage, Göteborg, 26 October 2001*; Center for Environment and Sustainability, Chalmers: Göteborg, Sweden, 2001.
11. Shafieifarhood, A.; Stewart, A.; Li, F. Iron-containing mixed-oxide composites as oxygen carriers for chemical looping with oxygen uncoupling (clou). *Fuel* **2015**, *139*, 1–10. [[CrossRef](#)]
12. Abad, A.; Cuadrat, A.; Mendiara, T.; García-Labiano, F.; Gayán, P.; de Diego, L.F.; Adánez, J. Low-cost Fe-based oxygen carrier materials for the IG-CLC process with coal. 2. *Ind. Eng. Chem. Res.* **2012**, *51*, 16230–16241. [[CrossRef](#)]
13. Mendiara, T.; Pérez, R.; Abad, A.; de Diego, L.F.; García-Labiano, F.; Gayán, P.; Adánez, J. Low-cost Fe-based oxygen carrier materials for the IG-CLC process with coal. 1. *Ind. Eng. Chem. Res.* **2012**, *51*, 16216–16229. [[CrossRef](#)]
14. Leion, H.; Mattisson, T.; Lyngfelt, A. Use of ores and industrial products as oxygen carriers in chemical-looping combustion. *Energy Fuels* **2009**, *23*, 2307–2315. [[CrossRef](#)]
15. Fossdal, A.; Bakken, E.; Øye, B.A.; Schøning, C.; Kaus, I.; Mokkelbost, T.; Larring, Y. Study of inexpensive oxygen carriers for chemical looping combustion. *Int. J. Greenh. Gas Control* **2011**, *5*, 483–488. [[CrossRef](#)]
16. Mendiara, T.; García-Labiano, F.; Gayán, P.; Abad, A.; de Diego, L.F.; Adánez, J. Evaluation of the use of different coals in chemical looping combustion using a bauxite waste as oxygen carrier. *Fuel* **2013**, *106*, 814–826. [[CrossRef](#)]
17. Acharya, B.; Dutta, A.; Basu, P. Chemical-looping gasification of biomass for hydrogen-enriched gas production with in-process carbon dioxide capture. *Energy Fuels* **2009**, *23*, 5077–5083. [[CrossRef](#)]
18. Arjmand, M.; Leion, H.; Mattisson, T.; Lyngfelt, A. Investigation of different manganese ores as oxygen carriers in chemical-looping combustion (CLC) for solid fuels. *Appl. Energy* **2014**, *113*, 1883–1894. [[CrossRef](#)]
19. Wen, Y.-Y.; Li, Z.-S.; Xu, L.; Cai, N.-S. Experimental study of natural Cu ore particles as oxygen carriers in chemical looping with oxygen uncoupling (clou). *Energy Fuels* **2012**, *26*, 3919–3927. [[CrossRef](#)]
20. Moldenhauer, P.; Rydén, M.; Lyngfelt, A. Testing of minerals and industrial by-products as oxygen carriers for chemical-looping combustion in a circulating fluidized-bed 300 W laboratory reactor. *Fuel* **2012**, *93*, 351–363. [[CrossRef](#)]
21. Frohn, P.; Arjmand, M.; Azimi, G.; Leion, H.; Mattisson, T.; Lyngfelt, A. On the high-gasification rate of brazilian manganese ore in chemical-looping combustion (CLC) for solid fuels. *AIChE J.* **2013**, *59*, 4346–4354. [[CrossRef](#)]

22. Velasco-Sarria, F.J.; Forero, C.R.; Arango, E.; Adánez, J. Reduction and oxidation kinetics of Fe–Mn-based minerals from southwestern Colombia for chemical looping combustion. *Energy Fuels* **2018**, *32*, 1923–1933. [[CrossRef](#)]
23. Velasco-Sarria, F.J.; Forero, C.R.; Adánez-Rubio, I.; Abad, A.; Adánez, J. Assessment of low-cost oxygen carrier in south-western Colombia, and its use in the in-situ gasification chemical looping combustion technology. *Fuel* **2018**, *218*, 417–424. [[CrossRef](#)]
24. Ortega Montero, C.R.; Rojas, E.E. Yacimientos minerales en Colombia. In *XII Congreso Colombiano de Geología; Congreso Las Geociencias: Paipa, Colombia*, 2009.
25. Leion, H.; Lyngfelt, A.; Johansson, M.; Jerndal, E.; Mattisson, T. The use of ilmenite as an oxygen carrier in chemical-looping combustion. *Chem. Eng. Res. Des.* **2008**, *86*, 1017–1026. [[CrossRef](#)]
26. Adánez, J.; Cuadrat, A.; Abad, A.; Gayán, P.; de Diego, L.F.; García-Labiano, F. Ilmenite activation during consecutive redox cycles in chemical-looping combustion. *Energy Fuels* **2010**, *24*, 1402–1413. [[CrossRef](#)]
27. Cuadrat, A.; Abad, A.; Adánez, J.; de Diego, L.F.; García-Labiano, F.; Gayán, P. Behavior of ilmenite as oxygen carrier in chemical-looping combustion. *Fuel Process. Technol.* **2012**, *94*, 101–112. [[CrossRef](#)]
28. Abad, A.; Adánez, J.; Cuadrat, A.; García-Labiano, F.; Gayán, P.; de Diego, L.F. Kinetics of redox reactions of ilmenite for chemical-looping combustion. *Chem. Eng. Sci.* **2011**, *66*, 689–702. [[CrossRef](#)]
29. Leion, H.; Jerndal, E.; Steenari, B.M.; Hermansson, S.; Israelsson, M.; Jansson, E.; Johnsson, M.; Thunberg, R.; Vadenbo, A.; Mattisson, T.; et al. Solid fuels in chemical-looping combustion using oxide scale and unprocessed iron ore as oxygen carriers. *Fuel* **2009**, *88*, 1945–1954. [[CrossRef](#)]
30. Abad, A.; Adánez, J.; García-Labiano, F.; de Diego, L.F.; Gayán, P.; Celaya, J. Mapping of the range of operational conditions for Cu-, Fe-, and Ni-based oxygen carriers in chemical-looping combustion. *Chem. Eng. Sci.* **2007**, *62*, 533–549. [[CrossRef](#)]
31. Mattisson, T.; Lyngfelt, A.; Cho, P. The use of iron oxide as an oxygen carrier in chemical-looping combustion of methane with inherent separation of CO₂. *Fuel* **2001**, *80*, 1953–1962. [[CrossRef](#)]
32. Jerndal, E.; Mattisson, T.; Lyngfelt, A. Thermal analysis of chemical-looping combustion. *Chem. Chem. Eng. Res. Des.* **2006**, *84*, 795–806. [[CrossRef](#)]
33. Cho, P.; Mattisson, T.; Lyngfelt, A. Defluidization conditions for a fluidized bed of iron oxide-nickel oxide-and manganese oxide-containing oxygen carriers for chemical-looping combustion. *Ind. Eng. Chem. Res.* **2006**, *45*, 968–977. [[CrossRef](#)]
34. Mattisson, T.; Johansson, M.; Lyngfelt, A. Multicycle reduction and oxidation of different types of iron oxide particles-application to chemical-looping combustion. *Energy Fuels* **2004**, *18*, 628–637. [[CrossRef](#)]
35. Rydén, M.; Cleverstam, E.; Johansson, M.; Lyngfelt, A.; Mattisson, T. Fe₂O₃ on Ce-, Ca-, or Mg-stabilized ZrO₂ as oxygen carrier for chemical-looping combustion using NiO as additive. *AIChE J.* **2010**, *56*, 2211–2220.
36. Cho, P.; Mattisson, T.; Lyngfelt, A. Carbon formation on nickel and iron oxide-containing oxygen carriers for chemical-looping combustion. *Ind. Eng. Chem. Res.* **2005**, *44*, 668–676. [[CrossRef](#)]
37. Mei, D.; Mendiara, T.; Abad, A.; de Diego, L.F.; García-Labiano, F.; Gayán, P.; Adánez, J.; Zhao, H. Evaluation of manganese minerals for chemical looping combustion. *Energy Fuels* **2015**, *29*, 6605–6615. [[CrossRef](#)]
38. Larring, Y.; Pishahang, M.; Sunding, M.F.; Tsakalakis, K. Fe–Mn based minerals with remarkable redox characteristics for chemical looping combustion. *Fuel* **2015**, *159*, 169–178. [[CrossRef](#)]
39. Stobbe, E.R.; de Boer, B.A.; Geus, J.W. The reduction and oxidation behaviour of manganese oxides. *Catal. Today* **1999**, *47*, 161–167. [[CrossRef](#)]
40. Zafar, Q.; Abad, A.; Mattisson, T.; Gevert, B.; Strand, M. Reduction and oxidation kinetics of Mn₃O₄/Mg-ZrO₂ oxygen carrier particles for chemical-looping combustion. *Chem. Eng. Sci.* **2007**, *62*, 6556–6567. [[CrossRef](#)]
41. Rydén, M.; Leion, H.; Mattisson, T.; Lyngfelt, A. Combined oxides as oxygen-carrier material for chemical-looping with oxygen uncoupling. *Appl. Energy* **2014**, *113*, 1924–1932. [[CrossRef](#)]
42. Källén, M.; Hallberg, P.; Rydén, M.; Mattisson, T.; Lyngfelt, A. Combined oxides of iron, manganese and silica as oxygen carriers for chemical-looping combustion. *Fuel Process. Technol.* **2014**, *124*, 87–96. [[CrossRef](#)]
43. Jing, D.; Arjmand, M.; Mattisson, T.; Rydén, M.; Snijkers, F.; Leion, H.; Lyngfelt, A. Examination of oxygen uncoupling behaviour and reactivity towards methane for manganese silicate oxygen carriers in chemical-looping combustion. *Int. J. Greenh. Gas Control* **2014**, *29*, 70–81. [[CrossRef](#)]
44. Mendiara, T.; Gayán, P.; Abad, A.; García-Labiano, F.; de Diego, L.F.; Adánez, J. Characterization for disposal of Fe-based oxygen carriers from a CLC unit burning coal. *Fuel Process. Technol.* **2015**, *138*, 750–757. [[CrossRef](#)]

45. García-Labiano, F.; Gayán, P.; Adánez, J.; de Diego, L.F.; Forero, C.R. Solid waste management of a chemical-looping combustion plant using cu-based oxygen carriers. *Environ. Sci. Technol.* **2007**, *41*, 5882–5887. [[CrossRef](#)] [[PubMed](#)]
46. UNE-EN-12457-3. *Caracterización de Residuos–Lixiviación–Ensayo de Conformidad Para la Lixiviación de Residuos Granulares y Lodos*; AENOR: Madrid, Spain, 2003; p. 35.
47. European Union. Council decision 2003/33/ec establishing criteria and procedures for the acceptance of waste at landfills pursuant to article 16 of and annex ii to directive 1999/31/ec. *Off. J. Eur. Union* **2003**, *L 11*, 27–49.
48. Arango, E.; Vasquez, F.G. *Determinación de los Parámetros Cinéticos Para la Combustión Usando Minerales del Suroccidente Colombiano Como Transportadores Sólidos de Oxígeno*; Universidad del Valle: Cali-Colombia, Colombia, 2016.
49. Gonzáles, D.A.; Parra, T.X. *Análisis de Reactividad de Materiales Basados en Cromita, Óxidos de Hierro y Óxidos de Manganeso Como Posibles Transportadores Sólidos de Oxígeno*; Universidad del Valle: Cali-Colombia, Colombia, 2015.
50. Mejía, A.F.; Jaramillo, C.C. *Análisis de Reactividad de Ilmenita y Olivino Como Posibles Transportadores Sólidos de Oxígeno en el Proceso Chemical Looping Combustion (CLC)*; Universidad del Valle: Cali-Colombia, Colombia, 2015.
51. Forero, C.R. *Combustión de Gas Con Captura de CO₂ Mediante Transportadores Sólidos de Oxígeno a Base de Cuo*; Universidad de Zaragoza-Consejo Superior de Investigaciones Científicas (CSIC): Zaragoza, España, 2011.
52. IDEAM. Protocolos de muestreo y análisis de laboratorio para la caracterización fisicoquímica de los residuos o desechos peligrosos en el país. In *Resolución 0062*; Instituto de Hidrología: Bogota, Colombia, 2007; Volume Resolución 0062.
53. Ministerio de Ambiente, Vivienda, y Desarrollo Territorial. *Decreto 4741 de Diciembre 30 de 2005*; Decreto 4741 de diciembre 30 de 2005; Ministerio de Ambiente: Bogotá, Colombia, 2005; p. 27.
54. Ministerio de Ambiente, Vivienda, y Desarrollo Territorial. *Gestión Integral de Residuos o Desechos Peligrosos. Bases Conceptuales*; Ministerio de Ambiente, Vivienda y Desarrollo Territorial, Dirección de Desarrollo Sectorial Sostenible/Organización de Control Ambiental y Desarrollo Empresarial OCADE: Bogotá, Colombia, 2007; p. 186.
55. Adánez Elorza, J.; de Diego Poza, L.F.; García Labiano, F.; Gayán Sanz, P.; Abad Secades, A. Material Transportador de O₂ Obtenible a Partir de CuO y MgAl₂O₄ y USO de Dicho Material en la Combustión de Sólidos con Captura Inherente de CO₂. Patente ES2390334 A1, 12 November 2012.
56. Mao, L.; Deng, N.; Liu, L.; Cui, H.; Zhang, W. Inhibition of Cr(III) oxidation during thermal treatment of simulated tannery sludge: The role of phosphate. *Chem. Eng. J.* **2016**, *294*, 1–8. [[CrossRef](#)]



© 2018 by the authors. Licensee MDPI, Basel, Switzerland. This article is an open access article distributed under the terms and conditions of the Creative Commons Attribution (CC BY) license (<http://creativecommons.org/licenses/by/4.0/>).